Available online at www.sciencedirect.com
SCIENCE DIRECT®
International Journal of Thermal Sciences 43 (2004) 561–568
International Journal of Thermal Sciences
www.elsevier.com/locate/ijts

Three-dimensional stationary thermal behavior of a bearing ball

A. Baïri *, N. Alilat, J.G. Bauzin, N. Laraqi

Department of Heat Transfer, University of Paris 10, LEEE, E.A. 387, 1, chemin Desvallières, 92410 Ville d'Avray, France

Received 12 May 2003; accepted 17 October 2003

Available online 7 January 2004

Abstract

A study of the temperature distribution in a bearing ball subjected to elliptic moving heat sources and surface cooling is presented in this paper. An explicit analytical solution is developed in order to determine the three-dimensional stationary temperatures in the ball. This allows the establishment of the thermal map of the ball, and the flash and average temperatures over the heated region regardless of the value of Peclet number. Two cases were considered: (i) uniform heat flux, (ii) parabolic heat flux. The flash temperature for the two thermal loading are compared as a function of Peclet number. Some results are also presented and discussed in order to show the effect of the motion and the cooling on the thermal behavior of the ball.

Keywords: Heat conduction in bearing ball; Hertzian contact; Elliptic contact; Moving heat sources

1. Introduction

The friction in ball bearings entails a heating of the balls that can have very detrimental effects. When applied to the aerospace or aeronautics fields the frictional heating can often be sudden and violent. The increase of temperature generated by these phenomena can involve mechanical microdeformations and an overheating of the cooling fluid (especially when dealing with cryogenic fluids). It is therefore important to have calculation models in order to evaluate the temperatures according to the frictional heat input, to which the solids are subjected. The calculation of temperature in the solids under friction has been of great scientific interest over the past few decades. Since the pioneering works (e.g., Boussinesq [1], Rosenthal [2], Blok [3], Jaeger [4] and Archard [5]) concerning semi-infinite solids which are adiabatic outside the region heated by a moving heat source, many other research studies have been conducted. They deal with cooled semi-infinite bodies (e.g., DesRuisseaux and Zerkle [6]), and with rotating cylinder subjected to a heat source and surface cooling (e.g., Ling and Simkins [7], DesRuisseaux and Zerkle [6], Gecim and Winer [8], Patula [9]). These research studies showed the evolution of flash temperatures (notion introduced by Blok [10]) according to the main characteristic parameters, i.e., Peclet and Biot numbers.

The case of an elliptic moving heat source on an insulated semi-infinite body has been studied by Francis [11], Bejan [12] and Tian and Kennedy [13] with asymptotic solutions. The analytical solutions are often difficult to get because of: (i) the non-homogeneous boundary conditions (localized heating and surface cooling), (ii) the relative motion (especially for the low values of Peclet number), and (iii) the small size of the contact region in relation to other dimensions of solid. From available studies, it is clearly shown that the increase of the Peclet number involves a decrease in temperature elevation over the contact region for a given heat flux.

The determination of the temperatures in a bearing requires a good knowledge of the thermal contact parameters and convective exchanges with the cooling fluid (e.g., Laraqi et al. [14], Bourouga et al. [15], Litsek and Bejan [16]).

The study which is proposed in this paper deals with the determination of the temperature in a bearing ball. The analytic calculation of the three-dimensional stationary temperature in a ball is addressed. In order to determine this analytic solution we proceed to a geometric transposition. The calculations are carried out in a Cartesian geometry. This transposition is consistent with the fact that the contact area is much smaller (about a few percent) than that of the

* Corresponding author.
E-mail address: dahmane.bairi@cva.u-paris10.fr (A. Baïri).

1290-0729/$ – see front matter
doi:10.1016/j.ijthermalsci.2003.10.008

Nomenclature

a, b	semiaxes of elliptical contact area
A, B	dimensions of the studied cell (see Fig. 2)
Bi	Biot number, $= hR/k$
$f(x, y)$	distribution of heat flux over the ellipse
h	heat convection coefficient
k	thermal conductivity
Pe	Peclet number, $= Va/2\alpha$
q_0	heat flux density
r	radius
R	radius of the ball
R_c	thermal constriction resistance
T	temperature
T^*	dimensionless temperature, $= T/(q_0 a/k)$
V	peripheral velocity
x, y, z	Cartesian coordinates

Greek symbols

α	thermal diffusivity
ε	surface ratio, $= \sqrt{\pi ab/4AB}$
ψ	dimensionless resistance, $= R_c k\sqrt{\pi ab}$

Subscripts

av	average
b	bulk
c	contact
f	flash

Superscripts

p	parabolic heat source
u	uniform heat flux

ball. It is again justified that the thermal penetration depth decreases with an increase in speed (or Peclet number). On the other hand, the elliptic geometry of the ball-ring contact area is taken into account. The developed analytical solution allows to establish the thermal map of the ball, and to determine the flash and average temperatures of the contact area. This solution is valid regardless of the value of Peclet number, and it may also be used in many other applications (gear, rollers, ...).

2. Assumptions of the model

The body under investigation is a sphere (see Fig. 1) subject to two elliptic uniform or parabolic heat sources diametrically opposite (simulating the contact with the two rings of a ball-bearing) and cooled on the rest of its surface. The heat convection coefficient is denoted h and the reference temperature is zero. The ball is in rotating motion around the axis indicated on this figure. The development of an analytical solution for the three-dimensional spherical geometry is complicated and requires the use of special functions which are difficult to manipulate. Considering the small size of the heated region in relation to the surface of the ball, it is widely justified to do the calculations in Cartesian geometry (Fig. 2). Indeed, the thermal depth penetration is much smaller than the radius of the ball, especially as the speed increases. Therefore, the effect of the curvature becomes negligible.

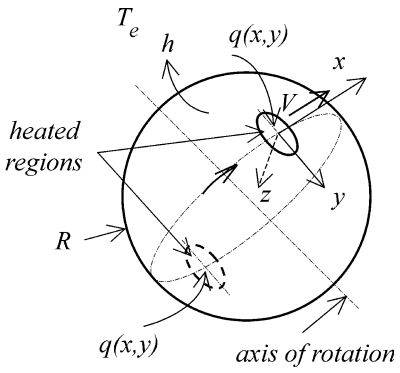

Fig. 1. Parameterization of a bearing ball.

The heat entering by the elliptic regions is entirely evacuated by the surface of the ball. One can assimilate the behavior of the ball to the one of a semi-infinite body. Therefore the choice of a finite body with an adiabatic boundary condition can be considered without difficulty. The two heat sources and the elliptic regions are assumed identical (this assumption is not restrictive), which permits to reduce the calculations to half of the domain (only one source with the conditions of periodicity). The physical properties of materials and the conditions of exchanges are assumed to be independent of the temperature.

3. Development of the model

On the basis of the above assumptions and of the notations of Fig. 2, the heat transfer in the body is governed by the following equations:

- heat equation

$$\frac{\partial^2 T}{\partial x^2} + \frac{\partial^2 T}{\partial y^2} + \frac{\partial^2 T}{\partial z^2} - \frac{V}{\alpha}\frac{\partial T}{\partial x} = 0 \tag{1}$$

- boundary conditions with respect to z-direction

$$-k\left(\frac{\partial T}{\partial z}\right)_{z=0} = \begin{cases} q_0 f(x, y) & (x/a)^2 + (y/b)^2 \leqslant 1 \\ -hT & \text{elsewhere} \end{cases} \tag{2}$$

$$\left(\frac{\partial T}{\partial z}\right)_{z\to\infty} = 0 \tag{3}$$

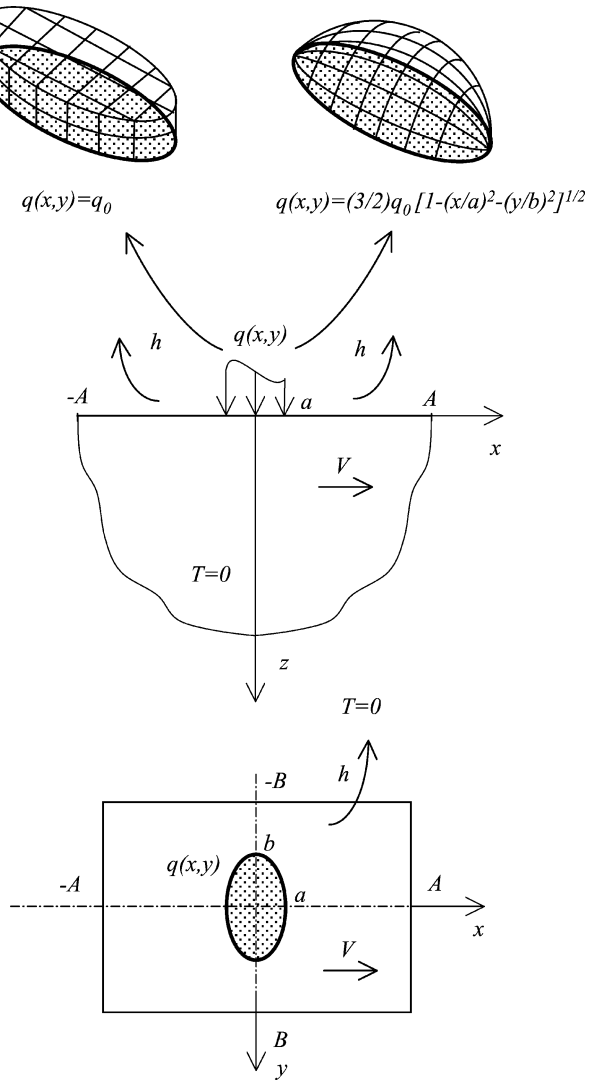

Fig. 2. Studied physical model.

- conditions of periodicity with respect to x-direction

$$(T)_{x=-A} = (T)_{x=A} \tag{4}$$

$$\left(\frac{\partial T}{\partial x}\right)_{x=-A} = \left(\frac{\partial T}{\partial x}\right)_{x=A} \tag{5}$$

- boundary conditions with respect to y-direction

$$\left(\frac{\partial T}{\partial y}\right)_{y=-B} = 0 \tag{6}$$

$$\left(\frac{\partial T}{\partial y}\right)_{y=B} = 0 \tag{7}$$

In Eq. (2), the function $f(x, y)$ denotes the distribution of heat flux over the ellipse. Two cases are studied in this paper:

(i) $f^u(x, y) = 1$, for the uniform heat flux, and
(ii) $f^p(x, y) = (3/2)[1 - [(x/a)^2 + (y/b)^2]]^{1/2}$ for the parabolic heat flux.

The factor $3/2$ in the expression of parabolic heat flux is due to the equality of total heat flux over the ellipse between the two studied distributions of heat as

$$\iint_{A_c} f^u(x, y)\,\mathrm{d}s = \iint_{A_c} f^p(x, y)\,\mathrm{d}s$$

(where A_c is the contact area).

The heat convection coefficient is difficult to determine in the configuration of a ball-bearing. However, on the basis of a numerical study of a roller bearing (Litsek and Bejan [16]) one can get an order of magnitude of this coefficient.

In order to solve the above governing equations, we use the following integral transforms:

$$\widetilde{T} = \frac{\varepsilon_m}{2A}\int_{-A}^{A} T\exp(-im\pi x/A)\,\mathrm{d}x \tag{8}$$

$$\widetilde{\widetilde{T}} = \frac{\varepsilon_n}{B}\int_{0}^{B} \widetilde{T}\cos(n\pi y/B)\,\mathrm{d}y \tag{9}$$

with $\varepsilon_{j=0} = 1$ and $\varepsilon_{j\neq 0} = 2$ ($j \equiv m$ or n).

The above integral transforms are especially appropriate to periodic systems (here, the heat diffusion with respect to $x-$direction) and symmetric conditions (here, the boundary conditions with respect to y-direction). Then, the governing Eqs. (1) to (7) lead to a simple differential equation of second order as

$$\frac{\mathrm{d}^2\widetilde{\widetilde{T}}}{\mathrm{d}z^2} - \left[\left(\frac{m\pi}{A}\right)^2 + \left(\frac{n\pi}{B}\right)^2 + im\pi\frac{V}{\alpha A}\right]\widetilde{\widetilde{T}} = 0 \tag{10}$$

$$-k\left(\frac{\mathrm{d}\widetilde{\widetilde{T}}}{\mathrm{d}z}\right)_{z=0} = q_0 G_{mn} - h\widetilde{\widetilde{T}} \tag{11}$$

$$\left(\frac{\mathrm{d}\widetilde{\widetilde{T}}}{\mathrm{d}z}\right)_{z\to\infty} = 0 \tag{12}$$

The expression of term G_{mn} in Eq. (11) depends of the thermal loading on the ellipse of contact (i.e., the expression of $f(x, y)$). Considering the two studied cases, we have

$$G^u_{mn} = \frac{\varepsilon_m\varepsilon_n}{2}\frac{\pi ab\,J_1\left[\sqrt{(m\pi a/A)^2 + (n\pi b/B)^2}\right]}{AB\sqrt{(m\pi a/A)^2 + (n\pi b/B)^2}} \tag{13}$$

for the case of uniform heat flux over the ellipse, and

$$G^p_{mn} = \frac{3\varepsilon_m\varepsilon_n}{4mB}\int_0^b \sqrt{1-(y'/b)^2}\,J_1\left[\frac{m\pi a}{A}\sqrt{1-(y'/b)^2}\right] \times \cos(n\pi y'/B)\,\mathrm{d}y' \tag{14}$$

for the case of parabolic heat flux over the ellipse.

The details of the determination of the above expressions of G_{mn} are given in the Appendix A.

In Eq. (11), considering the small value of the heated region with regard to that of the cell, we considered that the cooling is over the whole surface. This avoids getting

a solution under the integral equation (integral equation of Fredholm). Gecim and Winer [8] showed that this hypothesis is justified in the case of localized contacts (i.e., small ratio of the contact area to the apparent area) and when the heat coefficient is not very high. These conditions are verified in our application.

The general solution of Eq. (10) can be written as follows:

$$\tilde{\tilde{T}} = C_{00}z + D_{00} + C_{mn}e^{-\beta_{mn}z} + D_{mn}e^{\beta_{mn}z} \quad (\text{with } m, \text{ and/or, } n \neq 0) \tag{15}$$

where

$$\beta_{mn} = \rho_{mn}\exp(i\gamma_{mn}) \tag{16}$$

$$\rho_{mn} = \left[\left(\left(\frac{m\pi}{A}\right)^2 + \left(\frac{n\pi}{B}\right)^2\right)^2 + \left(\frac{m\pi V}{\alpha A}\right)^2\right]^{1/4} \tag{17}$$

$$\gamma_{mn} = \frac{1}{2}\tan^{-1}\left[\frac{(m\pi V/\alpha A)}{(m\pi/A)^2 + (n\pi/B)^2}\right] \tag{18}$$

Taking into account the boundary conditions, one gets

$$C_{00} = 0, \qquad D_{00} = \frac{q_0\pi ab}{4ABh}$$
$$C_{mn} = q_0\frac{G_{mn}}{\beta_{mn}k + h}, \qquad D_{mn} = 0 \tag{19}$$

The temperatures are determined by applying the inverse transforms, such as

$$\tilde{T} = \sum_{n=0}^{\infty}\tilde{\tilde{T}}\cos(n\pi y/B) \tag{20}$$

$$T = \Re\left\{\sum_{m=0}^{\infty}\tilde{T}\exp(im\pi x/A)\right\} \tag{21}$$

The final expression of temperature becomes

$$T = T_b + q_0\sum_{\substack{m=0\\n\neq 0}}^{\infty}\sum_{\substack{n=0\\m\neq 0}}^{\infty}\frac{G_{mn}}{\eta_{mn}} \times\cos\left[\frac{m\pi x}{A} - \varphi_{mn} - z\rho_{mn}\sin(\gamma_{mn})\right] \times\cos\left[\frac{n\pi y}{B}\right]e^{-z\rho_{mn}\cos(\gamma_{mn})} \tag{22}$$

with

$$T_b = \frac{q_0\pi ab}{4ABh} \tag{23}$$

$$\eta_{mn} = \sqrt{h^2 + k^2\rho_{mn}^2 + 2hk\rho_{mn}\cos(\gamma_{mn})} \tag{24}$$

$$\varphi_{mn} = \tan^{-1}\left[\frac{k\rho_{mn}\sin(\gamma_{mn})}{h + k\rho_{mn}\cos(\gamma_{mn})}\right] \tag{25}$$

In solution (22), the total temperature, $T(x, y, z)$, is the sum of ambient temperature, T_e (here $T_e = 0$), the bulk temperature, T_b (i.e., the first term of Eq. (22)), and the flash temperature, T_f (the last term of Eq. (22)). The bulk temperature, T_b, corresponds to the thermal balance between the heat flux dissipated by the source (i.e., $q_0\pi ab$) and the heat flux evacuated by convection (i.e., $4ABhT_b$). It is also the particular case when m and n are simultaneously equal to zero. Indeed, in the expressions of G_{mn}, given by Eqs. (13) and (14), we have

$$\lim\left[J_1(u)/u\right]_{u\to 0} = 1/2 \tag{26}$$

and $G_{mn}^{u,p}$ (for $m = 0$ and $n = 0$) becomes

$$G_{00}^{u,p} = \frac{\pi ab}{4AB} \quad (m = 0 \text{ and } n = 0) \tag{27}$$

4. Temperature profile

The numerical applications that are presented in this study are aimed at highlighting the configuration where the heated elliptic region is very small compared with the total surface of the ball (i.e., $\varepsilon \ll 1$). We choose the value $\varepsilon = 0.001$. The elongation of the ellipse is $b/a = 4$. These choices allow to limit the number of parameters to investigate.

4.1. Uniform heat flux

In a first step, the proposed solution is compared to Tian and Kennedy [13] results for a single circular source on an insulated semi-infinite body. The heat source is considered uniform. In the proposed model, we take $h = 0$, $a/b = 1$, $A/B = 1$, $\varepsilon = 0.001$. In this case the proposed solution is exact because $h = 0$ (i.e., no convection over the ball surface).The series requires 800 terms to converge for $\varepsilon = 0.001$, and this number decreases almost linearly when ε increases (until 200 terms for $\varepsilon = 0.01$). Table 1 provides the maximum dimensionless flash temperature T_f^* for three values of Peclet number (0.01, 1 and 10). The location $(x, 0, 0)$ of T_f^* depends of the Peclet value and the distribution of heat source (see Section 4.2). The relative difference between the two models, denoted Δ, is lower than 1.5%.

Fig. 3 shows the surface thermal map in the vicinity of the ellipse for two values of Peclet number $Pe = 0.2$ (a) and $Pe = 10$ (b), respectively. The graphs are plotted at the same

Table 1
Comparison of maximum dimensionless flash temperatures with Tian and Kennedy results [13] ($a = b$, $A = B$, $\varepsilon = 0.001$)

$Pe = Va/2a$		T_f^*		
		0.01	1	10
q^u	Eq. (22)	0.997	0.741	0.341
	From [13]	0.996	0.748	0.336
	Δ	0.1%	0.9%	1 .5%
q^p	Eq. (22)	1.152	0.852	0.374
	From [13]	1.173	0.876	0.391
	Δ	1.8%	2.8%	4.5%

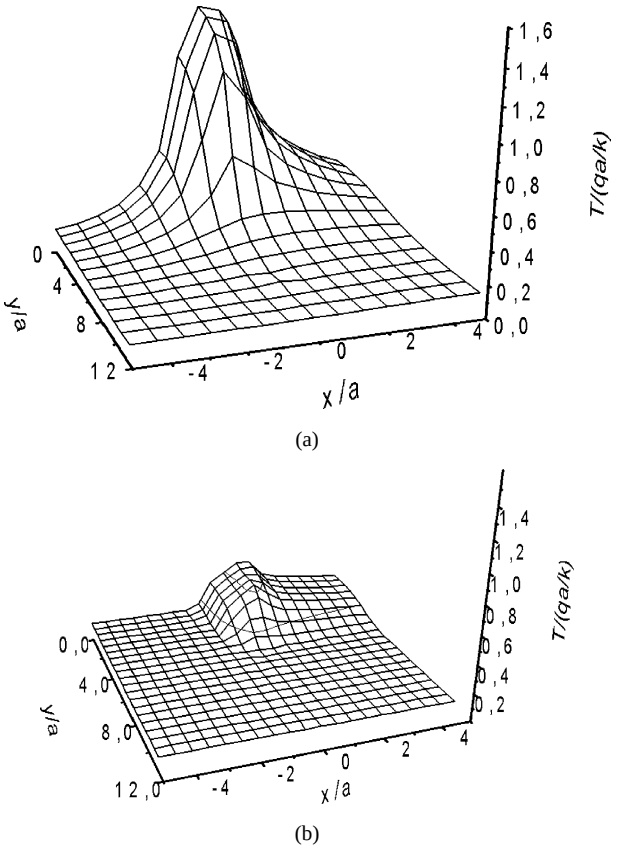

Fig. 3. Dimensionless total surface temperature at the vicinity of contact. (a) $Pe = 0.2$; (b) $Pe = 10$.

scale in order to be compared. These figures show the clear reduction of the dimensionless surface temperature with the increase of Peclet number for a given value of q_0. The region of the thermal gradients is located at the vicinity of the ellipse.

In order to verify the above assumption of geometric transposition of sphere to parallelepiped, the isothermal lines in the xz-plane for the same Peclet values as previously are drawn in Fig. 4. For the largest thermal penetration depth (i.e., small Peclet number value, here $Pe = 0.2$) the temperature is approximately divided by 8 between the surface and the depth $5a$. Practically, the order of magnitude of a is a few tens of μm, the thermal penetration depth is the order of a tenth of a millimeter.

The surface temperature along the axis of symmetry ($y = 0$) is reported on Fig. 5 for four values of the Biot number (0.008 , 0.04, 0.08 and 0.8) and four values of Peclet number (0.2, 1, 5 and 10). One finds for each case the usual curvature of the temperature profile due to a moving heat source. The flash temperature decreases with the increase of Peclet number and the abscissa of the maximum temperature moves from the center of the source (at $Pe \to 0$) to the exit (at $Pe \to \infty$). The temperatures decrease with the increase of Biot number. The rate of decrease is important between the values $Bi = 0.008$ and $Bi = 0.04$, and becomes smaller beyond this value (e.g., $Bi > 0.04$).

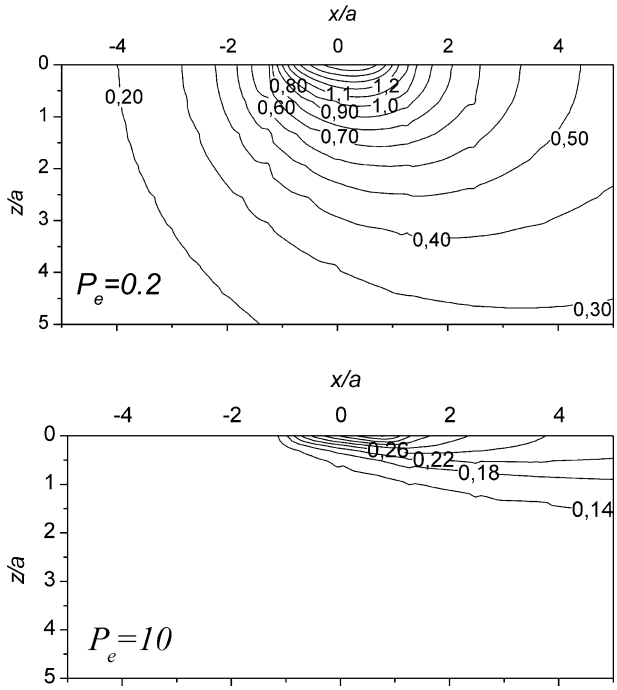

Fig. 4. Isothermal lines into the solid.

4.2. Parabolic heat flux

The maximum dimensionless flash temperatures given by the proposed solution are compared with those provided by Tian and Kennedy [13] for the case of a circular source with a parabolic heat flux. As previously, we take $h = 0$, $a/b = 1$, $A/B = 1$, $\varepsilon = 0.001$ in the proposed solution. Table 1 presents the results of comparison for three values of Peclet number (0.01, 1 and 10). The relative difference between the two models, Δ, is lower than 4.5%. This difference is essentially due to the uncertainty on the location of the maximum point on the temperature curves.

To compare the case of parabolic heat flux to the uniform one, Fig. 6 provides the evolution of dimensionless surface temperature for $Bi = 0.04$ and $Pe = 0.2$, 1, and 5. This figure shows that the maximum flash temperature is greater in the case of a parabolic heat flux and its location moves more slowly from the center of source to the exit when Pe increases.

5. Average temperature

The knowledge of the average surface temperature of the heated elliptic region is important for the study of the thermal constriction phenomena. We establish its expression by integration of the distribution of the surface temperature $T(x, y, 0)$ over the heated area, as

$$T_{\text{av}} = \frac{1}{\pi ab} \iint_{A_c} T(x, y, 0)\, \mathrm{d}x\, \mathrm{d}y \tag{28}$$

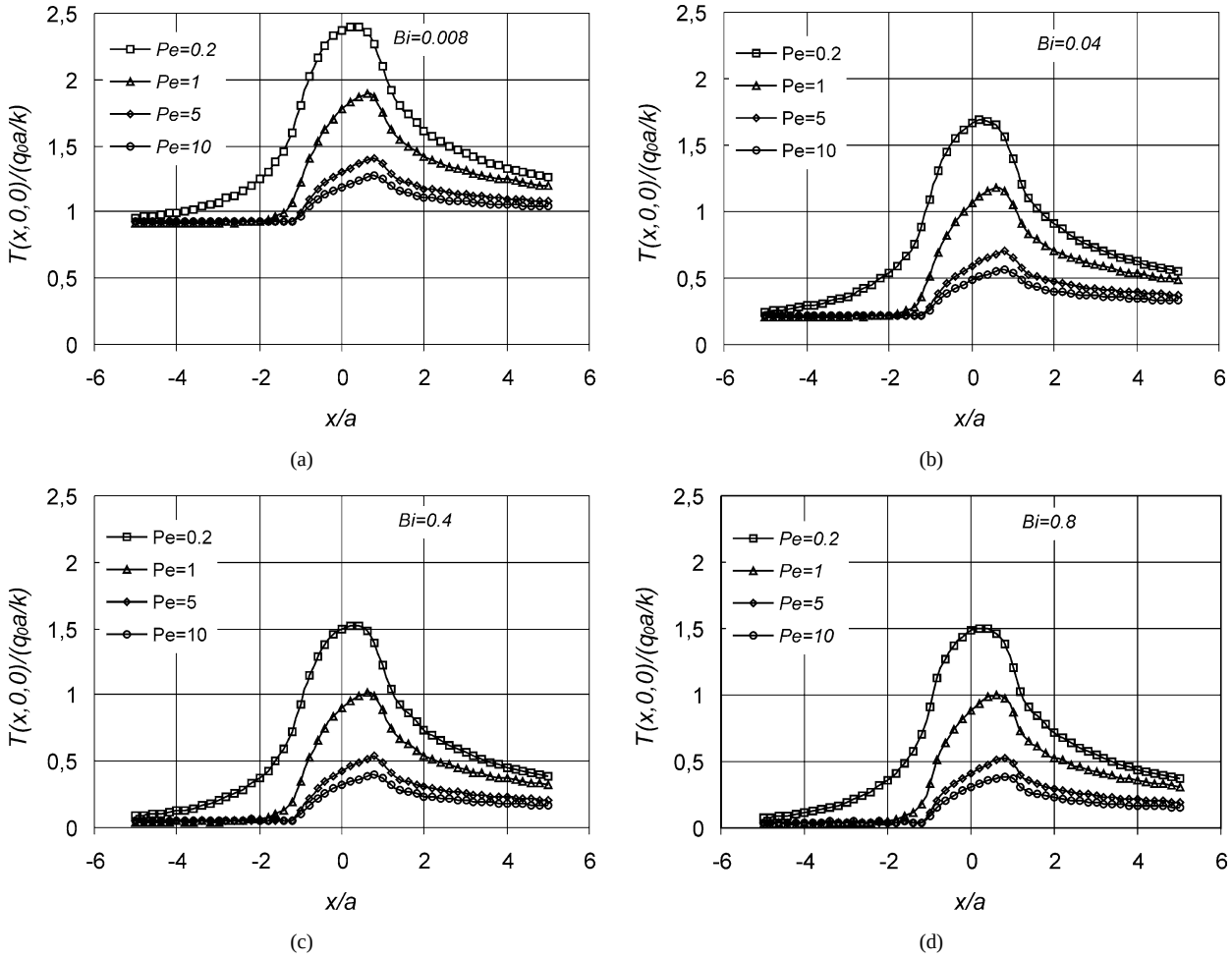

Fig. 5. Dimensionless total surface temperature along the axis of symmetry vs. *Bi* and *Pe*.

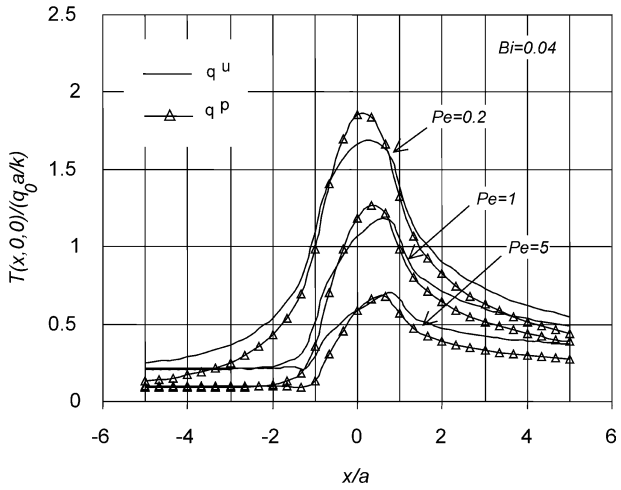

Fig. 6. Comparison between uniform and parabolic heat source as a function of *Pe* for $Bi = 0.04$.

The above integrations are the same nature as those of the function G which are detailed in Appendix A.

After calculation, we get the following expressions:

$$T_{\mathrm{av}}^{u} = T_b + \frac{q_0 \pi ab}{AB} \sum_{\substack{m=0 \\ n\neq 0}}^{\infty} \sum_{\substack{n=0 \\ m\neq 0}}^{\infty} \times \frac{\varepsilon_m \varepsilon_n \cos(\varphi_{mn}) J_1^2\left[\sqrt{(m\pi a/A)^2 + (n\pi b/B)^2}\right]}{\eta_{mn}\left[(m\pi a/A)^2 + (n\pi b/B)^2\right]} \tag{29}$$

for the uniform heat flux, and

$$T_{\mathrm{av}}^{p} = T_b + 2q_0 \sum_{\substack{m=0 \\ n\neq 0}}^{\infty} \sum_{\substack{n=0 \\ m\neq 0}}^{\infty} \times \frac{G_{mn}^{p} \cos(\varphi_{mn}) J_1\left[\sqrt{(m\pi a/A)^2 + (n\pi b/B)^2}\right]}{\eta_{mn}\sqrt{(m\pi a/A)^2 + (n\pi b/B)^2}} \tag{30}$$

for the parabolic heat source.

6. Hertzian contact with $\varepsilon \ll 1$ and $h = 0$

In an Hertzian contact, the contact area is usually much smaller than that of the ball (i.e., $\varepsilon \ll 1$) and the character-

istic dimensions are a and b. This configuration is similar to that of unique moving elliptic heat source.

If the Peclet number, *Pe*, is large (typically $Pe > 5$), the heat conduction can be neglected in the contact plane, and Eq. (1) becomes

$$\frac{\partial^2 T}{\partial z^2} - \frac{V}{\alpha}\frac{\partial T}{\partial x} = 0 \tag{31}$$

The problem becomes easy to solve (by using the Laplace transformation for example), and the average surface temperature can be written as

$$T^u_{\text{av}}(Pe \gg 1) = \frac{q_0 a}{k\sqrt{2}}\frac{1}{\sqrt{Pe}} \tag{32}$$

for a uniform heat flux.

The thermal constriction resistance, $R_c = (T^u_{\text{av}} - T_b)/(q_0 \pi a b)$, can be written as

$$R_c(Pe \gg 1) = \frac{1}{\pi\sqrt{2}}\frac{1}{kb}\frac{1}{\sqrt{Pe}} \tag{33}$$

Fig. 7 compares the evolution of the dimensionless constriction resistance, $\psi = R_c k\sqrt{\pi a b}$, between the exact solution, given by Eq. (29) (with $\varepsilon = 0.001$) and the asymptotic solution, given by Eq. (33). We have considered four values of the ratio a/b (0.1, 0.25, 0.5 and 1) and several values of *Pe*. The curvatures show that the two solutions depart below a certain value of Peclet number. This value seems to decrease with the increase of the ratio a/b. Otherwise, the constriction resistance decreases with the decrease of a/b and *Pe* values.

The particular case of a circular contact (i.e., $a = b$) has been studied by Archard [5] for a large value of Peclet number, and by Tian and Kennedy [13] with an asymptotic development for any value of Peclet number. The values of ψ calculated by the present solution and the Tian and Kennedy [13] correlation are in agreement as shown in Table 2.

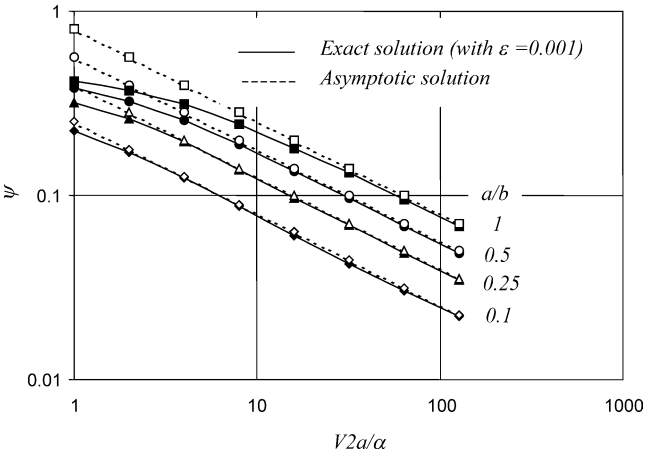

Fig. 7. Dimensionless constriction resistance for a single elliptic moving contact.

Table 2
Comparison of dimensionless constriction resistance with Tian and Kennedy results [13] ($a = b$, $A = B$, $\varepsilon = 0.001$)

$V2a/\alpha$	ψ	
	Eq. (29), with $\varepsilon = 0.001$	From [13]
0	0.4752	0.4789
1	0.4162	0.4077
2	0.3718	0.3610
4	0.3110	0.3017
8	0.2434	0.2383
16	0.1816	0.1800

7. Conclusion

An analytical solution was presented in this paper in order to determine the thermal behavior of a bearing ball subjected to uniform or parabolic heat source, on an elliptic region. By adopting the two following assumptions: (i) small dimension of the contact area compared with the surface of the ball (i.e., low thermal penetration depth), (ii) the cooling concerns the whole surface of the ball (including that of the application of the heat source), we may get an explicit analytical solution. This solution is valid regardless the value of Peclet number. This allows the establishment of the thermal map of the ball and the flash and average temperatures of the heated region. The results of the proposed solutions are in agreement with available published research results.

Appendix A. Details of calculation of G_{mn}

Eq. (2) gives the boundary condition at ($z = 0$) with a heat flux applied to the elliptic region. We apply the integral transforms (8) and (9) to the elliptic region as follows:

$$G_{mn} = \frac{\varepsilon_m \varepsilon_n}{2AB}\int_0^b \cos(n\pi y'/B)\,\mathrm{d}y' \times \int_{-a\sqrt{1-(y'/b)^2}}^{a\sqrt{1-(y'/b)^2}} f(x', y')e^{-im\pi x'/A}\,\mathrm{d}x' \tag{A.1}$$

A.1. Case of uniform heat flux as:

$$f^u(x', y') = 1 \tag{A.2}$$

The integration with respect to x-direction gives

$$G^u_{mn} = \frac{\varepsilon_m \varepsilon_n}{m\pi}\frac{1}{B}\int_0^b \sin\left[\frac{m\pi a}{A}\sqrt{1-(y'/b)^2}\right] \times \cos(n\pi y'/B)\,\mathrm{d}y' \tag{A.3}$$

The above integral is provided in Gradshteyn and Ryzhik [17]. We get the expression of G^u_{mn} under the following explicit form:

$$G^u_{mn} = \frac{\varepsilon_m \varepsilon_n}{2} \frac{\pi ab\, J_1\left[\sqrt{(m\pi a/A)^2 + (n\pi b/B)^2}\right]}{AB\sqrt{(m\pi a/A)^2 + (n\pi b/B)^2}} \tag{A.4}$$

A.2. Case of parabolic flux as:

$$f^p(x', y') = \frac{3}{2}\sqrt{1 - \left[(x'/a)^2 + (y'/b)^2\right]} \tag{A.5}$$

The integration with respect to x-direction gives

$$G^p_{mn} = \frac{3\varepsilon_m \varepsilon_n}{4mB} \int_0^b \sqrt{1 - (y'/b)^2}\, J_1 \times \left[\frac{m\pi a}{A}\sqrt{1 - (y'/b)^2}\right] \cos(n\pi y'/B)\, \mathrm{d}y' \tag{A.6}$$

No explicit solution for the above integral was found. It has to be solved numerically.

References

[1] J. Boussinesq, Calcul des températures successives d'un milieu homogène et atherme indéfini que sillone une source de chaleur, C. R. 110 (1890) 1242–1244.

[2] D. Rosenthal, Etude théorique du régime thermique pendant la soudure à l'arc, C. R. 2 (1935) 1277–1292.

[3] H. Blok, Les températures de surface dans des conditions de graissage sous extrême pression, in: Proc. Sd. World Petrol. Congr., vol. 3, 1937, pp. 471–486.

[4] J.C. Jaeger, Moving sources of heat and the temperature at sliding contacts, Proc. Royal Soc. of New South Wales 76 (1942) 203–224.

[5] J.F. Archard, The temperature of rubbing surfaces, Wear 2 (1958) 438–455.

[6] N.R. DesRuisseaux, R.D. Zerkle, Temperature in semi-infinite and cylindrical bodies subject to moving heat sources and surface cooling, ASME J. Heat Transfer (1970) 456–464.

[7] F.F. Ling, T.E. Simkins, Measurement of pointwise juncture condition of temperature at the interface of two bodies in sliding contact, ASME J. Basic Engrg. 85 (1963) 481–486.

[8] B. Gecim, W.O. Winer, Steady temperature in a rotating cylinder subject to surface heating and convective cooling, ASME J. Tribology 106 (1984) 120–127.

[9] E.J. Patula, Steady-state temperature distribution in a rotating roll subject to surface heat fluxes and convective cooling, ASME J. Heat Transfer 103 (1981) 36–41.

[10] H. Blok, Flash temperature concept, Wear 6 (1963) 483–493.

[11] H.A. Francis, Interfacial temperature distribution within a sliding Hertzian contact, ASLE Trans. 14 (1970) 41–54.

[12] A. Bejan, Theory of rolling contact heat transfer, ASME J. Heat Transfer 111 (1989) 257–263.

[13] X. Tian, F.E. Kennedy, Maximum and average flash temperatures in sliding contacts, ASME J. Tribology 116 (1994) 167–174.

[14] N. Laraqi, A. Bounagui, J. Bransier, Modélisation des transferts de chaleur dans un roulement à rouleaux cylindriques, Revue Française de Mécanique 3 (1994) 223–227.

[15] B. Bourouga, J.M. Briot, J.P. Bardon, Influence de la vitesse et de la charge sur la conductance thermique de transport entre les bagues d'un roulement à rouleaux, Int. J. Thermal Sci. 40 (7) (2001) 622–637.

[16] P.A. Litsek, A. Bejan, Convection in the cavity formed between two cylindrical rollers, ASME J. Heat Transfer 112 (1990) 625–631.

[17] I.S. Gradshteyn, I.M. Ryzhik, Table of Integrals Series and Products, Academic Press, New York, 1965.